***International Journal of Minerals*, *Metallurgy and Materials***
***Volume 21*, *Number 12*, *December 2014*, *Page 1241***
**DOI: 10.1007/s12613-014-1033-3**

# Comparative study of 2mol% Li- and Mn-substituted lead-free potassium sodium niobate ceramics

*Asha Dahiya*[1], *O.P. Thakur*[1], *J.K. Juneja*[2], *Sangeeta Singh*[3], *and Dipti*[3,4]

1) School of Applied Sciences, Netaji Subhas Institute of Technology, Dwarka University of Delhi, New Delhi-110078, India.
2) Department of Physics, Hindu College, Sonepat-131001, India
3) Department of Physics, Geeta Vidya Mandir Girls College, Sonepat-131001, India
4) School of Physics & Material Sciences, Thapar University, Patiala-147004, India

(Received: 10 February 2014; revised: 21 May 2014; accepted: 28 May 2014)

**Abstract:** The effect of Li and Mn substitution on the dielectric, ferroelectric and piezoelectric properties of lead free $K_{0.5}Na_{0.5}NbO_3$ (KNN) was investigated. Samples were prepared using a conventional solid state reaction method. The sintering temperature for all the samples was 1050°C. The optimum doping concentration for the enhancement of different properties without the introduction of any other co-dopants such as Ti, Sb, and La was investigated. X-ray diffraction analysis confirmed that all the samples crystallize in a single phase perovskite structure. The dielectric properties were investigated as a function of temperature and applied electric field frequency. Compared with Li-substituted KNN (KLNN), Mn-substituted KNN (KMNN) exhibited a higher dielectric constant $\varepsilon_{\max}$ (i.e., 4840) at its critical transition temperature $T_c$ (i.e., 421°C) along with a lower value of tangent loss at 10 kHz and greater values of saturation polarisation $P_s$ (i.e., 20.14 μC/cm$^2$) and remnant polarisation $P_r$ (i.e., 15.48 μC/cm$^2$). The piezoelectric constant ($d_{33}$) of KMNN was 178 pC/N, which is comparable to that of lead-based hard ceramics. The results presented herein suggest that B-site or Mn substitution at the optimum concentration results in good enhancement of different properties required for materials used in memory devices and other applications.

**Keywords:** ceramics; dielectric properties; ferroelectricity; piezoelectricity; substitution; comparative study

## 1. Introduction

Ferroelectric materials are a special class of piezoelectric materials used in capacitors and non-volatile memory devices. Because of their good piezoelectric, pyroelectric, and dielectric properties, these materials are also used in numerous other applications including actuators and sensors. Lead-based compounds, such as lead zirconate titanate (PZT) and some substituted compositions of PZT near the morphotropic phase boundary (MPB) are used for micro-electro mechanical systems because of their high piezoelectric constant, high electromechanical coupling coefficient and other ferroelectric properties [1]. However, PZT-based ceramics are highly hazardous for environment because PbO evaporates during the sintering process [2–6]. Therefore, the development of lead free ceramics has become an important issue to researchers.

Among lead-free materials such as barium titanate (BT), bismuth sodium titanate (BNT), bismuth strontium titanate (BST) and bismuth layer-structure ferroelectrics (BLSF), potassium sodium niobate (KNN) has been observed to be the most promising candidate. KNN has a high Curie temperature (greater than 400°C), good ferroelectric properties, and large electromechanical coupling factors. However, controlling the stoichiometry of hard KNN ceramics during their preparation via conventional sintering is very difficult due to the volatile nature of potassium. Oxygen deficiency is another problem during high temperature processing [7].

The hot-pressing technique and spark plasma sintering can be used to prepare materials with excellent piezoelectric properties and high densities [8–9]. However, such processing techniques are not appropriate for industrial applications. The doping of elements such as Sb, Ta, Sr, and La with

Corresponding author: Asha Dahiya E-mail: ashadh8@gmail.com

other suitable co-dopants into KNN is known to improve the density and electrical properties of KNN.

The effect of Li ($(K_{0.5}Na_{0.5})_{(1-x)}Li_xNbO_3$, KLNN) and Mn ($K_{0.5}Na_{0.5}Mn_xNb_{1-x}O_3$, KMNN) on the density and electrical properties of KNN with $x$ = 2mol%, 4mol%, and 6mol% has been studied in detail. The optimal value of substitution in both series with comparison of properties such as density and grain size was observed to be $x$ = 2mol%. In this study, the comparison of the properties of KLNN and KMNN for $x$ = 2mol% reveals the superiority of KMNN (B-site substitution) over KLNN (A-site substitution) for use in various applications.

## 2. Experimental

The oxides and carbonates (99.9% by assay) of the corresponding metals, i.e., $Na_2CO_3$, $K_2CO_3$, $Nb_2O_5$, $Li_2CO_3$, and $MnO_2$ were used as starting materials for the synthesis of KNN and substituted KNN ceramics via solid state route. Before being weighed, the powders were dried at 200°C for 4 h to remove any moisture and were subsequently stored in desiccators. The mixing and grinding process of weighed powders was carried out via wet ball milling in a high-energy planetary ball mill for 4 h using zirconia balls, and ethanol was used as milling medium. The slurry was subsequently dried at 200°C. The samples were subsequently calcined at 850°C for 3 h in an alumina crucible to decompose the carbonates. The dried powders were again ball milled and dried. A small amount of diluted polyvinyl alcohol (by 2wt%) was added as a binder and the mixtures were pressed into circular discs of 1 mm in thickness and 15 mm in diameter using a uniaxial hydraulic press. The discs were placed on a piece of platinum foil and sintered at 1050°C for 3 h with a heating/cooling rate of 5°C/min. The experimental density of the sintered pellets was determined using the Archimedes principle.

The crystal structure was determined by X-ray diffraction (XRD) analysis on a Bruker D-8 advanced model equipped with Cu $K_\alpha$ radiations source ($\lambda$ = 0.15406 nm). To measure the dielectric, ferroelectric and piezoelectric properties, the sintered pellets were lapped using alumina powder, and electrodes were subsequently painted using silver paste, on the flat surface of the pellet. The samples were heated at 500°C for 30 min to ensure good ohmic contacts. The dielectric properties as a function of temperature (30–500°C) at 1, 10, and 100 kHz were measured using an Agilent 4263B LCR meter. Polarization vs. electric field ($P$–$E$) hysteresis loops were recorded at 20 Hz at room temperature using an automated $P$–$E$ loop tracer based on the Sawyer–Tower circuit. The samples were poled in a silicon bath at 100°C by applying a field of 1.5 kV/mm for 1 h and then cooled to room temperature. The piezoelectric properties were measured using a quasistatic piezoelectric coefficient test meter.

## 3. Result and discussion

### 3.1. Structural properties

Fig. 1 shows the XRD patterns of the KNN, KLNN, and KMNN ceramics synthesized at 1050°C. At room temperature, all of the samples exhibited a single-phase perovskite structure with orthorhombic symmetry. With the substitution of Li and Mn into the structure, the diffraction peaks in the $2\theta$ range of 40°–50° slightly shifted toward higher angles. The cell parameters were calculated from the XRD patterns using the Bragg's equation, i.e., $2d\sin\theta = n\lambda$ where $n$ = 1. The results are presented in Table 1. The increase in the $c/a$ ratio suggests that the tetragonality increased for KLNN and KMNN. The relative density for all of the samples was calculated to be greater than 80%, as shown in Table 1. A comparison of the densities reveals that the maximum density after sintering was attained in the case of Mn-substituted samples. $MnO_2$ acts as a sintering aid and introduces the liquid phase during the sintering process, which results in the higher density of the Mn-substituted KNN sample [9–10] as shown in Fig. 2(a). Because Li is volatile by nature, it may evaporate during sintering and create voids; such voids reduce the density of the Li-substituted KNN sample, as shown in Fig. 2(b).

### 3.2. Dielectric properties

Fig. 3 shows the variation in dielectric constant with temperature at three frequencies (1, 10, and 100 kHz) for KNN, KLNN, and KMNN. These graphs indicate that the

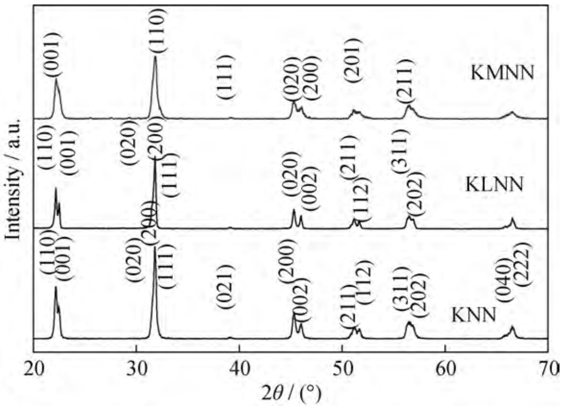

**Fig. 1. XRD patterns of the KNN, KLNN, and KMNN samples.**

**Table 1. Variation of relative density, cell parameters (*c* and *a*), transition temperature ($T_c$), room-temperature dielectric constant ($\varepsilon_{RT}$), maximum dielectric constant at the transition temperature ($\varepsilon_{max}$), and tangent loss at the transition temperature ($\tan\delta_{max}$) for different samples at 10 kHz**

| Sample | Relative density / % | $c$ / nm | $a$ / nm | $T_c$ / °C | $\varepsilon_{RT}$ | $\varepsilon_{max}$ | $\tan\delta_{max}$ |
|---|---|---|---|---|---|---|---|
| KNN | 83.89 | 0.3959 | 0.3907 | 403 | 395 | 2485 | 0.078 |
| KLNN | 81.53 | 0.3956 | 0.3894 | 437 | 380 | 2545 | 0.590 |
| KMNN | 85.84 | 0.3972 | 0.3892 | 421 | 800 | 4840 | 0.102 |

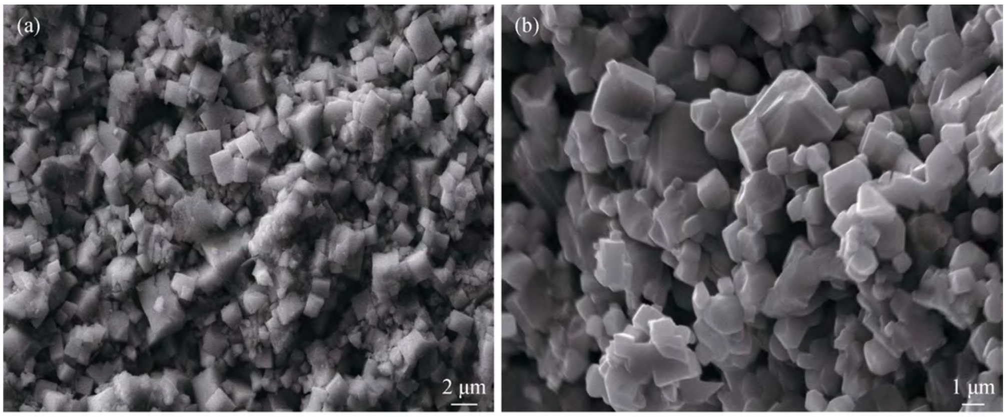

Fig. 2. SEM micrographs of KNN: (a) Mn-substituted; (b) Li-substituted.

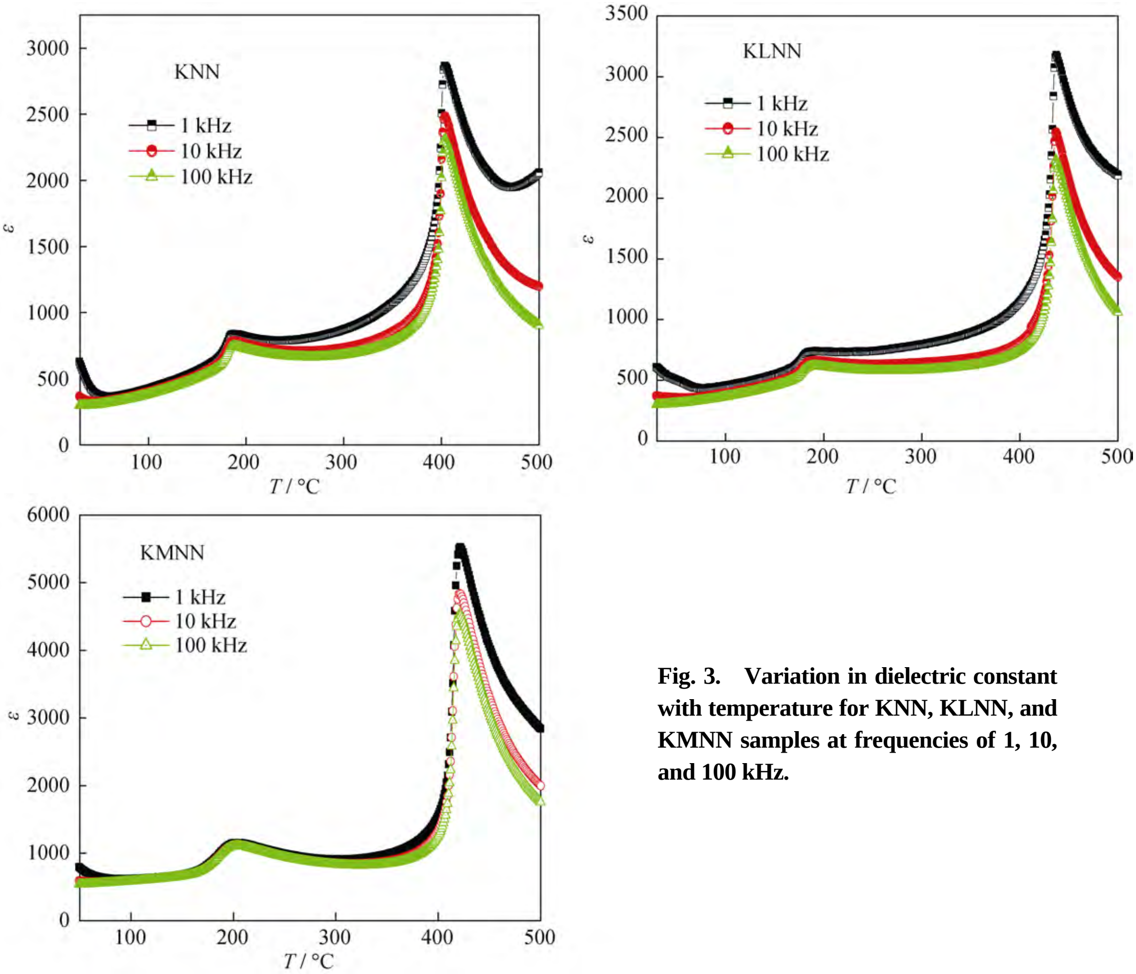

Fig. 3. Variation in dielectric constant with temperature for KNN, KLNN, and KMNN samples at frequencies of 1, 10, and 100 kHz.

dielectric constant initially increased with increasing temperature, reached a maximum value at the ferroelectric Curie temperature ($T_c$) and subsequently decreased with further increase in temperature. The behavior of the dielectric constant as a function of temperature for all three samples reveals two phase transitions: one from orthorhombic to tetragonal and the other from tetragonal to cubic, with the first transition occurring approximately at 200°C. The observed behavior is in agreement with behavior reported for KNN-based samples synthesized by different methods [11–13]. The increase in dielectric constant at higher temperatures is due to an increase in dielectric polarization in the material. For the pure KNN sample, at lower frequencies there is an increase in dielectric constant with further increase in temperature in the paraelectric region. This behavior might be related to low frequency relaxation process [14]. The dispersion of the dielectric constant was clearly observed over a wide range of temperature near the Curie temperature in the cases of KNN and KLNN; this dispersion was due to microstructural inhomogeneities and interatomic short range molecular forces. However, the dispersion was much less pronounced in the case of KMNN, which reflects the homogeneity of the sample.

Fig. 4 shows the temperature dependence of the dielectric constant and the tangent loss at 10 kHz for all of the samples. The higher values of the tangent loss at higher temperatures are attributed to thermal conductivity losses. The values of the relative density, cell parameters ($c$ and $a$), ferroelectric Curie temperature ($T_c$), room temperature dielectric constant ($\varepsilon_{RT}$), dielectric constant at $T_c$ ($\varepsilon_{max}$), and loss tangent at $T_c$ ($\tan\delta_{max}$) at 10 kHz for all three samples are given in Table 1. The first transition temperature did not substantially change after Li and Mn were substituted in KNN; however, the Curie temperature shifted towards higher values. The increase in the Curie temperature may be due to the generation of internal stresses up on the substitution of other elements into pure KNN; it is also related to the tetragonality of the samples. As the tetragonality of the samples increases, the transition temperature will increase. The maximum dielectric constant and minimum tangent loss were observed for KMNN as compared to KLNN and pure KNN.

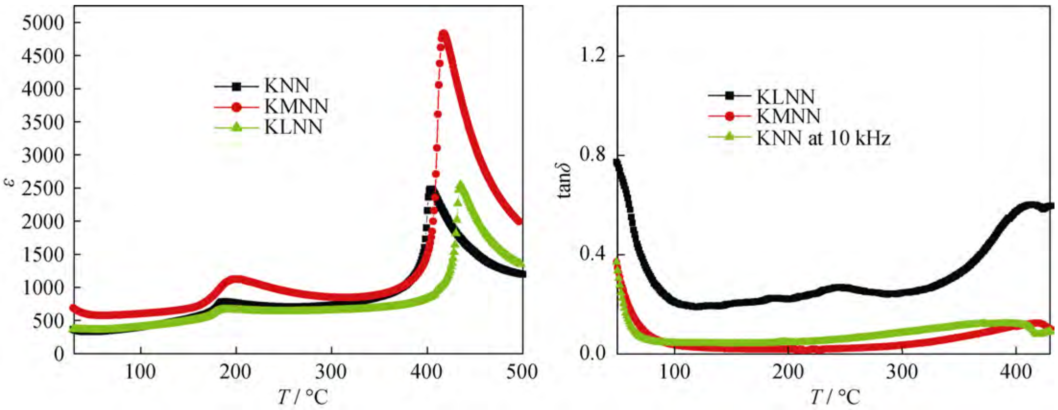

**Fig. 4. Comparison of dielectric constant (ε) and tangent loss (tanδ) with increasing temperature at 10 kHz for KNN, KLNN, and KMNN.**

The Li-substituted sample also exhibited an increase in dielectric constant and an increase in the Curie temperature compared with those of pure KNN; similar results have been reported by other researchers [15]. A high tangent-loss value was observed in the case of the Li-subsituted sample. These high tangent-loss values are attributed to the volatile nature of alkali elements at higher tempeatures; these voids enhance the leakage current in the sample. The above results indicate that KMNN, or B-site substitutesd KNN, is more suitable for dielectric applications.

The variation of the dielectric constant and the tangent loss with frequency at room temperature was also investigated for all of the samples; the results are shown in Fig. 5. High dielectric constant values were observed at lower frequencies, possibly because of space charge polarization. The decrease in dielectric constant with increasing frequency is rapid because as the frequency increases, the ionic and orientation polarization decreases [16]. Similar behavior with increasing frequency was observed in the case of the tangent loss. The values at room temperature indicate that the dielectric constant and loss tangent are minimized in the case of Li-substituted KNN, consistent with previous explanation as shown in the inset of Fig. 5.

### 3.3. Ferroelectric properties

Fig. 6 shows room temperature *P–E* hysteresis loops for

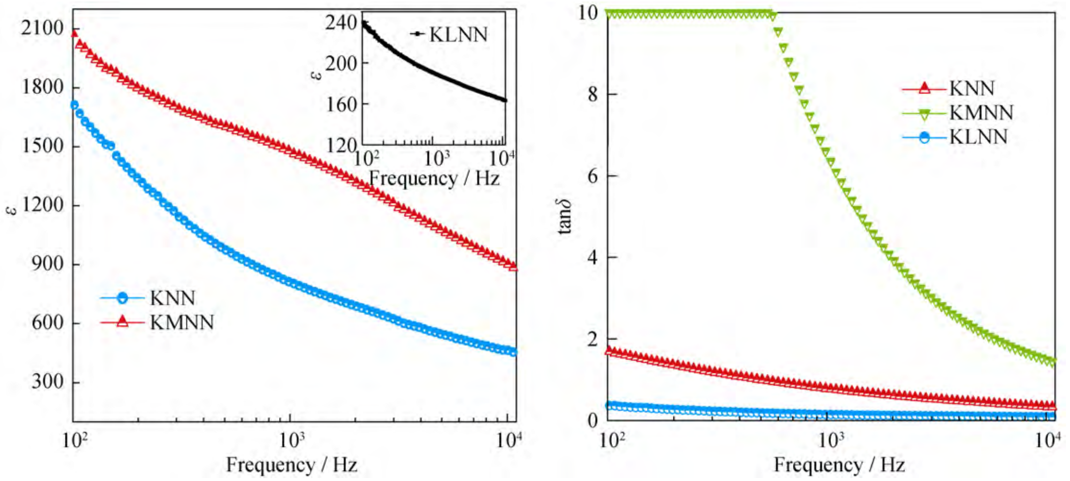

**Fig. 5. Variation in dielectric constant ($\varepsilon$) and tangent loss ($\tan\delta$) for all three samples as the frequency increased from 100 Hz to 10 kHz at room temperature.**

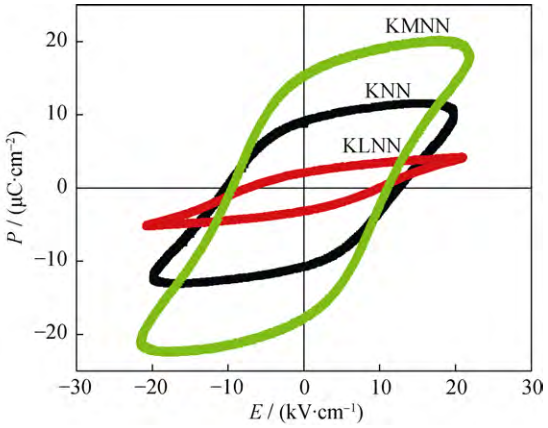

**Fig. 6. Ferroelectric *P–E* hysteresis loops of KNN, KLNN, and KMNN at 20 kV/cm.**

all of the samples, these hysteresis loops confirm the ferroelectric behavior of the samples. A comparison of the *P–E* loops reveals that both remnant polarization ($P_r$) and saturation polarization ($P_s$) increased in the case of the Mn-substituted sample; however, these values decreased in the case of the Li-substituted sample. The coercivity was not substantially affected by substitution of Mn or Li. The squareness ratio ($P_r/P_s$) also decreased upon substitution of Li. In the case of the KLNN sample, the ferroelectric behavior was weakened because of the sample's low internal polarizability [17–18]. The squareness ratios are given in Table 2.

### 3.4. Piezoelectric constant

The piezoelectric coefficients $d_{33}$ of the KNN and KLNN samples were found to be 80 pC/N and 147 pC/N, respectively. However, the maximum value (178 pC/N) was observed in the case of the KMNN ceramic poled under the same conditions.

**Table 2. Variation of the remnant polarization ($P_r$), saturation polarization ($P_s$), and squareness ratio ($P_r/P_s$) for KNN, KLNN, and KMNN**

| Sample | $P_r$ / (μC·cm$^{-2}$) | $P_s$ / (μC·cm$^{-2}$) | $P_r/P_s$ |
|---|---|---|---|
| KNN | 9.01 | 11.53 | 0.78 |
| KMNN | 15.48 | 20.14 | 0.76 |
| KLNN | 3.27 | 5.43 | 0.60 |

## 4. Conclusions

Li- and Mn-substituted potassium sodium niobate ceramics were prepared via a conventional solid-state reaction route. XRD analysis reveals that all of the samples were well crystallized into perovskite structures. The dielectric properties were measured as a function of temperature, and experimental results showed that the transition temperature $T_c$ varied among the three samples. All of the samples exhibited well defined ferroelectric behavior. The overall comparison reveals that A-site substitution in KNN leads to a higher inhomogeneity in KNN; as a result, desirable properties for memory devices are not achieved. However, B-site or Mn substitution results in a high value of remnant polarization $P_r$ (15.48 μC/cm$^2$) and a high piezoelectric cofficient $d_{33}$ (178 pC/N) which are very good for memory device applications.

## References

[1] M. Ichiki, L. Zhang, M. Tanaka, and R. Maeda, Electrical properties of piezoelectric sodium–potassium niobate, *J. Eur. Ceram. Soc.*, 24(2004), No. 6, p. 1693.

[2] T. Maeda, N. Takiguchi, M. Ishikawa, T. Hemsel, and T. Morita, (K,Na)NbO$_3$ lead-free piezoelectric ceramics synthe-

sized from hydrothermal powders, *Mater. Lett.*, 64(2010), No. 2, p. 125.

[3] M.R. Yang, C.C. Tsai, C.S. Hong, S.Y. Chu, and S.L. Yang, Piezoelectric and ferroelectric properties of CN-doped $K_{0.5}Na_{0.5}NbO_3$ lead-free ceramics, *J. Appl. Phys.*, 108(2010), No. 9, art. No. 094103.

[4] H. Ursič, A. Bencan, M. Skarabot, M. Godec, and M. Kosec, Dielectric, ferroelectric, piezoelectric, and electrostrictive properties of $K_{0.5}Na_{0.5}NbO_3$ single crystal, *J. Appl. Phys.*, 107(2010), No. 3, art. No. 033705.

[5] W. Yang, Z. Zhou, B. Yang, R. Zhang, Z. Wang, H. Chen, and Y. Jiang, Structure and piezoelectric properties of Fe-doped potassium sodium niobate tantalate lead-free ceramics, *J. Am. Ceram. Soc.*, 94(2011), No. 8, p. 2489.

[6] F. Gao, L. Liu, B. Xu, G.X. Hu, X. Cao, R. Hong, and C. Tian, Texture development and dielectric relaxor behavior of $0.80Na_{0.5}Bi_{0.5}TiO_3$–$0.20K_{0.5}Bi_{0.5}TiO_3$ ceramics templated by plate-like $NaNbO_3$ particles, *J. Eur. Ceram. Soc.*, 31(2011), No. 15, p. 2987.

[7] S.Y. Chu, W. Water, Y.D. Juang, J.T. Liaw, and S.B. Dai, Piezoelectric and dielectric characteristics of lithium potassium niobate ceramic system, *Ferroelectrics*, 297(2003), p. 11.

[8] R.P. Wang, R.J. Xie, T. Sekiya, and Y. Shimojo, Fabrication and characterization of potassium–sodium niobate piezoelectric ceramics by sparks-plasma-sintering method, *Mater. Res. Bull.*, 39(2004), No. 11, p. 1709.

[9] R. Rani, S. Sharma, R. Rai, and A.L. Kholkin, Investigation of dielectric and electrical properties of Mn doped sodium potassium niobate ceramic system using impedance spectroscopy, *J. Appl. Phys.*, 110(2011), No. 10, art. No. 104102.

[10] L.G. Gusakova, V.M. Ishchuk, N.G. Kisel, D.V. Kuzenko, and N.A. Spiridonov, Modified potassium–sodium niobate based lead-free piezoceramics, *Funct. Mater.*, 17(2010), No. 4, p. 528.

[11] I. Smeltere, M. Antonova, A. Kalvane, O. Grigs, and M. Livinsh, The effect of dopants on sintering and microstructure of lead-free KNN ceramics, *Mater. Sci.*, 17(2011), No. 1, p. 62.

[12] S.C. Bhatt, K. Singh, M. Uniyal, O. Prakash, P.K. Singh, R. Sexena, and B.S. Semwal, Temperature dependence of dielectric properties of sodium potassium niobate ceramics, *Indian J. Pure Appl. Phys.*, 45(2007), p. 609.

[13] J.B. Lim, Y.H. Jeong, M.H. Kim, D. Suvorov, and J.H. Jeon, Effect of K/Na ratio on piezoelectric properties of modified $(K_{1-x}\,Na_x)NbO_3$ “Hard” lead-free piezoelectrics, *Ceram. Int.*, 38(2012), No. 3, p. 2605.

[14] O.P. Nautiyal, S.C. Bhatt, R.P. Pant, and B.S. Semwal, Dielectric properties of silver sodium niobate mixed ceramic system, *Indian J. Pure Appl. Phys.*, 48(2010), No. 5, p. 357.

[15] S. Wongsaenmai, S. Ananta, and R. Yimnirun, Effect of Li addition on phase formation behavior and electrical properties of $(K_{0.5}Na_{0.5})NbO_3$ lead free ceramics, *Ceram. Int.*, 38 (2012), No. 1, p. 147.

[16] B. Jaffe, W.R. Cook Jr., and H. Jaffe, *Piezoelectric Ceramics*, Academic Press, New York, 1971, p.72.

[17] K. Uchino, *Ferroelectric Devices*, CRC Press, New York, 2000, p. 126.

[18] R. Rani, S. Sharma, R. Rai, and A.L. Kholkin, Doping effects of Li–Sb content on the structure and electrical properties of $[(Na_{0.5}\,K_{0.5})_{1-x}(Li)_x(Sb)_x(Nb)_{1-x}O_3]$ lead-free piezoelectric ceramics, *Mater. Res. Bull.*, 47(2012), No. 2, p. 381.